MILLIMETER-WAVE STRUCTURES AND POWER SOURCES

H. Henke, Technische Universitaet, 10587 Berlin, Germany

Abstract

Accelerators at millimeter wavelength are of increasing interest. Technological progress and new applications are the driving forces behind. The paper reports on developments for RF structures and power sources.

1 INTRODUCTION

In the last few years the development of millimeter-wave components was driven from both ends: New fabricational technologies and new applications. Micromechanic technology has developed advanced fabricational methods like high precision stamping, diamond turning, laser cutting, diffusion-bonding, electro-discharge machining (EDM), uv-lithography and deep x-ray lithography (LIGA). The applications cover very different areas such as linear colliders (LC), table-top accelerators and radiation sources, communication technology, magnetic resonance imaging, high resolution radar, electron cyclotron heating and control of fusion plasma and ceramic sintering. Some of the applications, for instance the last two, do not require phase stable signals and the adequate power sources are oscillators. Other applications, and in particular accelerators, need small band sources with high phase stability and therefore amplifiers. This paper presents some developments of high-power mm-wave amplifiers and accelerating structures as they are needed for accelerator applications.

2 ACCELERATING STRUCTURES

At around 100 GHz the typical structure dimensions are in the millimeter or submillimeter range. Classical round structures will need large openings for a good vacuum conductivity and will thus be difficult to construct and be very expensive. A more adequate geometry is a planar double-sided geometry, Fig. 1, as proposed in [1]. It is perfectly suited for fabrication by lithography and can easily be cooled at the top and the bottom. The side openings provide a natural possibility for vacuum pumping and for brazing or bonding the two halves together, because the RF-fields decay exponentially in the openings and the joint is field-free. They also allow for an easy damping of higher order modes. On the other hand, the RF fields in a planar structure have quadrupole character and one either has to control the effect or one takes advantage of it and uses it for focusing.

2.1 Traveling-Wave Constant Impedance Structure

This is probably the simplest possible structure and is the one shown in Fig. 1. It can be viewed as an iris loaded groove guide. The basic geometrical and RF parameters for the $2\pi/3$-mode at 91,39 GHz are given in [2] and repeated in Table 1.

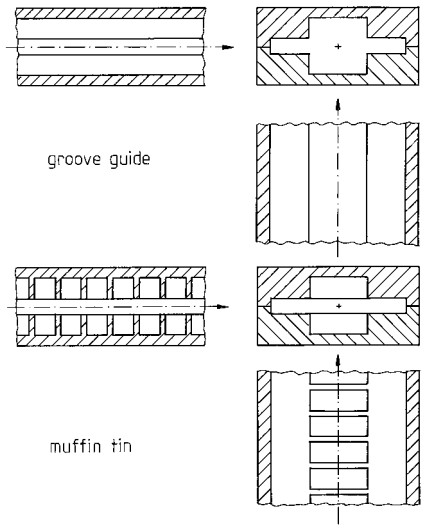

Figure 1: Basic arrangement of planar structures

Table 1: Geometrical and RF-parameters for a $2\pi/3$ TW-mode in the structure of Fig.1.

g = 0.864 mm	t = 0.230 mm	2a = 1.05 mm,
2 b = 2.54 mm,	w = 2.363 mm	
r/Q_0 = 81.6 kΩ/m,	Q_0 = 2490 for copper	
r_0 = 200 MΩ/m,	v_g/c_0 = 9.4 %	
α = 4.1 m–1	$\rightarrow$ L = 14.6 cm,	N = 133 for αL = 0.6

A similar structure with slightly different parameters was first constructed and measured at SLAC [3], [4]. It was a cold test seven-cell model consisting of five layers which were individually machined by wire EDM.

The central layer carries a ladder structure which forms the cavities once it is closed at top and bottom. It has also the beam port and a pumping slot. Two thin layers above and below will close the cavities and will provide matching irises for the power couplers. The three layers are clamped between two thick backing plates with incorporated waveguide tapers. Thus the vertical input/output scheme allows for an individual matching of the coupling irises. The layers were registered by precision alignment pins and clamped with screws and belleville washers. The machining accuracy was assessed to be around 2.5 µm variation in cavity size and within 1 µm deviation of nominal centers of cavities.

For RF measurements a home-made vector network analyzer was constructed. The reflection and transmission coefficients are shown in Fig. 2. They were in good

qualitative agreement with the simulations except for the magnitude of the transmission coefficient. An unexpected power loss of about 50 % in the passband was found.

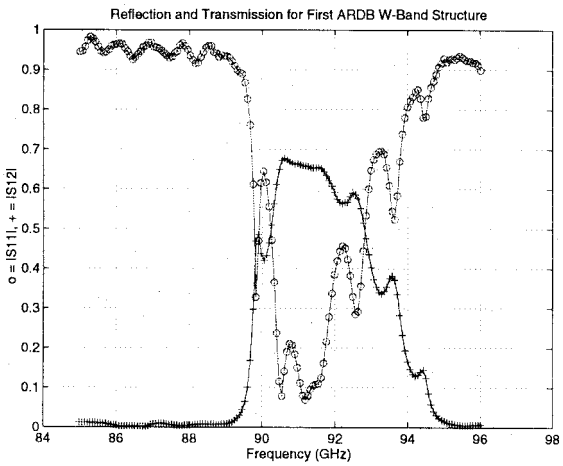

Figure 2: Measured reflection and transmission coefficient of the SLAC structure.

After the promising results of the EDM machined protopye in SLAC a second prototype was fabricated for the Technical University of Berlin [2] and Fig. 3.

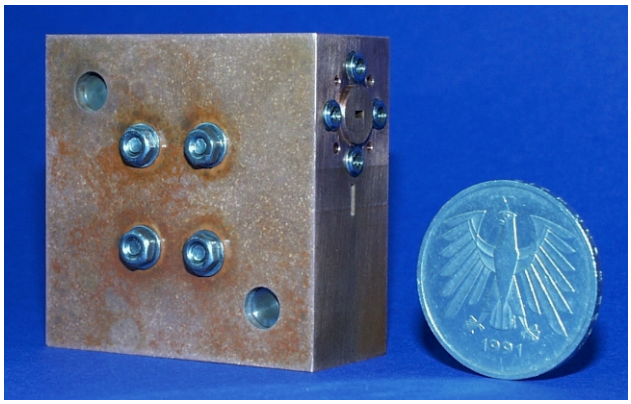

Figure 3: Prototype with RF flange and bolts.

The design differed from the first SLAC design in an essential point. The input/output coupling was done in the horizontal plane. This required bent feeding tapers coming from the two sides, and the matching irises had to be cut down by EDM with an oblique wire. The reasons for this choice were twofold: Firstly, a design which is suited for lithography and, secondly, a simplified mechanical arrangement were the layers with the coupling iris are no longer necessary.

As for the first prototype the mechanical accuracy was quite good, around 2 µm. For the RF measurements a home-made scalar network analyzer and a high-precision bead pull stand were constructed. The measured reflection and transmission coefficients as well as the field distribution showed good qualitative agreement with numerical simulations. But the transmission in the passband lacked again half of the power.

Several attempts at SLAC to improve the contacts between cell vanes and backing plates have failed so far. To mitigate the problem a structure was designed where no conducting joints were allowed between vanes and any other parts of the structure. That is e.g. a planar structure with the side walls of the cells omitted [11]. This structure has been dubbed zipper structure.

Simulations showed that the shunt impedance is poor and that an upper band overlaps with the fundamental band. Nevertheless, it was decided to build the structure because of the big advantage that no vane had to be brazed or bonded. Colt test measurements confirmed the calculated passband. The measured reflection showed appreciable differences as compared to simulations indicating that due to mechanical errors neither the match nor the bandwidth were well-achieved.

The fabrication by wire EDM was chosen because it is a relatively cheap process and it meets essentially the required tolerances. Thus, prototypes could be produced quickly and the concept of a two-sided planar structure was proven alright. However, wire EDM imposes a construction in layers which have to be brazed or diffusion bonded together. While this is state of the art for solid metal pieces, experiments at SLAC were unsuccessful up to now for connecting the thin, about 200 - 300 µm thick, irises to their ground plate. A process where one slab with cavities, matching iris and feeding guide can be fabricated in one go is deep x-ray lithography, called LIGA [5]. In a first lithographic step a thick resist layer of plastic is glued on a copper support plate and irradiated through a mask by synchrotron radiation. By developing the exposed resist layer, the template is produced which can be filled by electroplating copper on the support. After etching the unexposed resist away a microstructure is obtained. A third and fourth step allow for mass fabrication. A negative of the microstructure is obtained by injection moulding of thermoplastic material. The negative serves as a template for subsequent electroforming processes. Many structures can thus be made from the original masterpiece. Today LIGA is an advanced technology. The achievable accuracy is around 1 µm or better and structure depths of up to 1 mm are possible. This is exactly what is needed for planar mm-wave structures.

The Advanced Photon Source, Argonne, [6], has been working on the construction of structures and RF undulators with LIGA for several years and the Technical University Berlin [7] (see also next chapter) built a first home-made prototype and a second prototype in collaboration with the Synchrotron Radiation Research Center, Taiwan, [8]. Initial problems related with the resist material, the adhesion of the resist and internal stresses developing cracks are overcome. The electroplated copper has a level of oxygen which is too high and work is going on to develop plating of oxygen-free copper and dispersion hardened copper. The assessment of the mechanical accuracy, surface roughness and electrical data is on the way.

2.2 Double-Periodic Standing Wave Structures

For many applications, as in cw-operation or in storage rings, an sw-structure is needed. It has the advantage of a constant power dissipation but the shunt impedance is only half that of a TW-structure, except for the π-mode. For the π-mode, however, the mode spacing is small and only a small number of cells can be coupled. Also, the structure is very sensitive against dimensional errors and has phase errors from cell to cell.

A nice trick to overcome these problems is often used in proton machines. The accelerating cells are not coupled directly but via coupling cells, in such a way that the structure is operated in the π/2-mode but the effective phase advance from main to main cell is π. This is an effective but very expensive way to fabricate standard structures. In the case of planar structures and fabrication by lithography the solution is given for free. Two different arrangements have been investigated: A side-coupled structure (SCS) [9] and an on-axis-coupled structure (OACS) [10], Fig. 4.

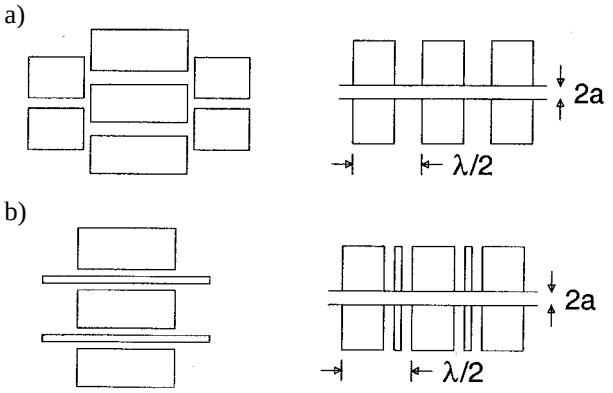

Figure 4: Top-view and cross-section of a) side-coupled structure and of b) on-axis coupled structure.

Both devices have coalescent pass-bands at π phase advance per cell. The dispersion diagram is symmetric around this point and has a large slope, that means there are no 1st-order cell-to-cell phase errors and the group velocity is high. Although the paper design and scaled-up models of the SCS behaved reasonably well the group velocity was relatively low and the dispersion diagram too much distorted. Better results were obtained for the OACS, which was finally chosen and designed with end cells and power coupler. The attenuation parameter was chosen as $\alpha L = 0.12$ yielding a structure length of 6.5 cm with 39 main cells. After verification of the design with scaled-up models a LIGA fabricated prototype was constructed, Fig. 5.

2.3 High Power Structure Tests

Since the access to high power sources at mm-wavelengths is difficult SLAC prepared a test where the structures were driven by a bunched beam at subharmonic

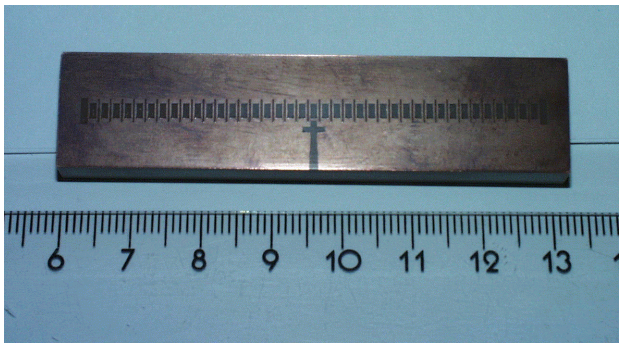

Figure 5: One half of an on-axis coupled structure fabricated with LIGA.

frequency [12]. The next linear collider test accelerator (NLCTA) which is bunched at 11.4 GHz and contains typically 1000 bunches in a pulse can be used as the 8th subharmonic driver for 91.4 GHz. Three experiments were performed. The first was with a single cell. The beam created 1kW RF power in the cavity corresponding to 25 MV/m gradient. No particular events could be observed. The second and third experiment were performed with a dielectric structure. It consisted of two horizontally arranged power couplers, two coupling cells, and the accelerating cells were replaced by a rectangular ceramic rod. The relative dielectric constant was 9.5, the Q-value was 1100 and the group velocity 11% of velocity of light. Measurements of the reflection and transmission coefficient, phase advance and attenuation confirmed well the simulations. The structure length was one inch. When the matched structure was driven by the beam it created up to 17 kW RF power corresponding to an accelerating gradient of 7 MV/m. Finally, the power coming out of the structure was fed back to the input with the right phase thus forming a recirculating scheme. In that case the beam created up to 175 kW power and a gradient of 18 MV/m.

3. POWER SOURCES

Power sources for accelerators are normally small-band devices with a high phase stablity. These are amplifiers, and the working horse up to today is the klystron. Its suprising and uninterrupted success is due to separated functions: The gun, where the continuous beam is created, an input RF circuit, which impresses a velocity modulation on the beam, a drift length for bunching, an output RF circuit, which extracts the power and a beam collector. The device is arranged in a linear channel with external magnetic focussing. During the more than 60 years since the birth of the klystron an unimaginable amount of different devices has been invented, but apart from particular applications none has succeeded as the klystron. Even in the range of mm-waves the klystron is still in the race although it has a strong competitor now, the gyroklystron.

3.1 Klystron

Two basic limitations exist on the power that can be generated by a conventional klystron [13]. First of all, the perveance

$$K = I_0 / U_0^{3/2} \quad (1)$$

measures the space charge forces and the RF component of the beam. It determines the efficiency η. A second limitation is related to the beam area, which depends on the wavelength. Typically, the beam radius should not be larger than λ/8. If one puts all factors together, the maximum output power is

$$P_{RF} \approx \frac{\pi}{64} \eta U_0 J_0 C_a \lambda^2 \quad (2)$$

with U_0 dc beam voltage, J_0 current density at the cathode and Ca the ratio of the beam area on the cathode to the area in the drift region. For a good cathode lifetime the current density should be less than about 10 A/cm^2. Then, with an area compression of 100 equ. (2) indicates a maximum power of about 200 kW at 90 GHz for a 100 kV beam voltage and an efficency of 40 %. Even if this number may be too optimistic and only 100 kW is achievable one could still power two structures, as given in Table 1, and obtain a voltage gain of 2 MV over 30 cm with an average gradient of 6.7 MV/m. But equ. (2) also shows the unfavorable scaling law for high frequencies, i.e. small wavelengths. To obtain very high powers one has to circumvent the area limit and go to a flat sheet-beam (next chapter) or an annular beam or multiple beams.

A modular klystron consisting of several klystrons on single substrate was studied at SLAC [14]. It was planned to fabricate the RF circuit with LIGA and to focus the beam by periodic permanent magnet (PPM) channels. The individual 'klystrinos' operating at U_0 = 120 kV, I_0 = 2.5 A with 125 kW RF power were arranged in parallel to form a module and several modules can be stacked to form a 'brick'. The outputs of the klystrinos were combined quasi-optically with mirrors.

The idea of independent modular klystrinos was modified later on in favor of arranging six klystrinos on a circle and having a common vacuum envelope [15]. The advantages are a single high voltage seal assembly and output window and a much better pumping of the gun, output cavity and collector areas. The entire devices is about 12 inches long, with 6-inch diameter. The combined output power is expected to be 750 kW with 35 % overall efficiency and 40 to 50 dB gain. In order to phase the six klystrinos correctly each input phase and amplitude will be controlled by microprocessors in relation of the output signal thus forming a 'smart tube'. The design and construction of the tube have started.

In a first model two klystrinos are on a common support; Fig. 6, with the RF circuit fabricated by LIGA and with the housing for the PPM structure.

First RF circuit prototypes are machined with EDM and with LIGA in collaboration with the SRRL [8]. Experiments with a beam tester are in progress.

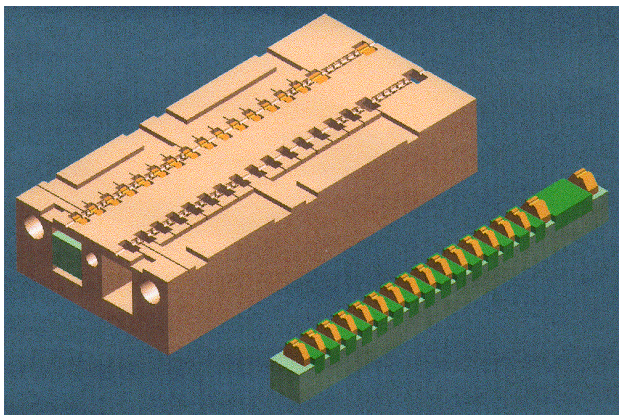

Figure 6: Models for 2 klystrinos with LIGA fabricated RF circuit and assembly.

3.2 Sheet-Beam Klystron (SBK)

As an alternative to multiple-beam klystrons one can increase the beam current in an SBK by making the beam much wider than thick.

The Technical University Berlin [16] worked on a paper design of an average power SBK. The design philosophy was rather having many cheap tubes of modest power instead of fewer high power devices. This would not only be better for microfabrication but also facilitate the power distribution. The tube had low voltage, U_0 = 30 kV, and a modulating anode so that the power supply would also be small and cheap. The RF circuit was designed for fabrication with LIGA and the beam was focused in a PMM channel. While some problems inherent in the RF circuits were solved, the efficiency of the tube could not be brought to a sufficiently high level. The reasons were a low circuit impedance due to the low voltage and the wide beam.

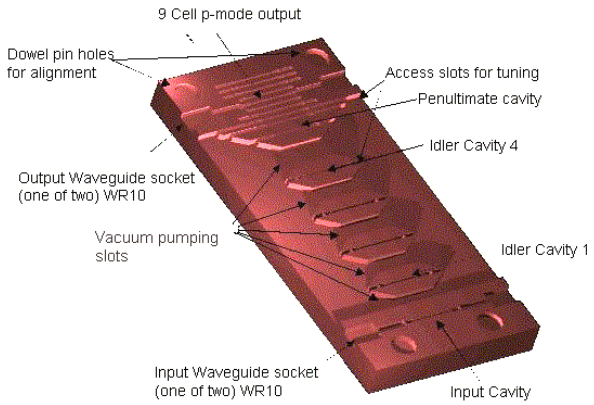

Figure 7: Sheet-beam klystron RF circuit.

At SLAC an SBK of higher voltage, U_0 = 140 kV, and RF power is under development [17]. Three-dimensional simulations of a PPM channel and a wiggler focusing have shown the validity of both concepts with a slight advantage for wiggler focusing. The RF circuit design is based on so-called 'barbel' cavities and the drift tube is

slotted with SiC RF absorbers in order to suppress mode propagation. Again, the geometry is chosen such that it is suitable for fabrication with LIGA, Fig. 7.

3.3 Gyroklystron

In gyroklystrons the beam interacts with the electromagnetic fields via its transverse velocity components and not with the longitudinal components as in klystrons. The electrons leave the cathode with a strong transverse velocity component and start spiraling, Fig. 8, with the cyclotron frequency. In an input cavity with an azimuthal electric field (TE mode) some electrons are accelerated, others decelerated depending on their position with respect to the electric field. This translates into an azimuthal bunching after a certain drift length. The bunching process and with it the gain can be increased by adding more cavities separated by drift spaces. In an output resonator, the azimuthally bunched beam is continuously decelerated and transfers energy to a TE-mode which is coupled out axially. The advantage of the scheme as compared to klystrons is that the beam area is annular and larger because the cavities can be operated in a higher order mode with a larger diameter. Therefore, gyroklystrons are particularly suited for high frequencies. The disadvantage is a more complex and inherently more unstable process.

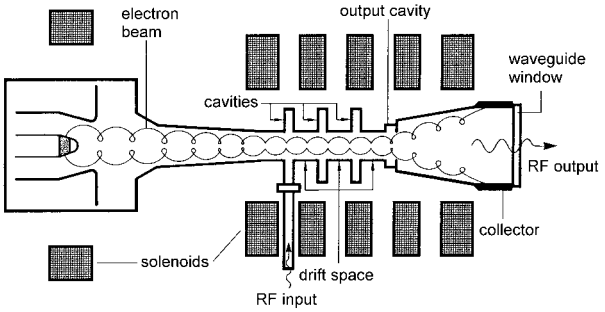

Figure 8: Schematic of a gyroklystron amplifier.

Gyroklystrons were successfully built, and at 93 GHz they produced between 60 and 70 kW power with efficiencies of 25 % or above [18]. The tubes were stable with a bandwidth between 460 and 640 MHz. Predictions from simulations and the measured results were in excellent agreement.

A very high power gyroklystron is under development [19]. The tube has U_0 = 500 kV, I_0 = 55 A and should produce 10 MW RF power at 91.39 GHz with 56 dB gain and an efficiency of 37 %. It is a second harmonic gyroklystron. The paper design is nearly finished and the tube is under construction.

REFERENCES

[1] H. Henke, Y.W. Kang, and R.L. Kustom, "A mm-wave RF structure for relativistic electron acceleration", Argonne National Laboratory ANL/APS/MMW-1, 1993.

[2] R. Merte, H. Henke, and R. Apel, "Design, fabrication and RF measurement of a w-band accelerating structure", PAC 1999,Vol. 2, pp. 818-20.

[3] P.J. Chou et al., "Design and fabrication of a traveling-wave muffin-tin accelerating structure at 90 GHz", SLAC-PUB-7498, May 1997.

[4] P.J. Chou et al., "RF measurements of a traveling-wave muffin-tin accelerating structure at 90 GHz", SLAC-PUB-7499, May 1997.

[5] E.W. Becker, W. Ehrfeld, P. Hagman, A. Maurer and D. Münchmeyer, Microelectronic Engineering, No. 4, 1986, pp. 35 -56.

[6] J.J. Song et al., "MM-wave cavity/klystron developments using deep x-ray lithography at the advanced photon source.", APAC 1998 KEK proceedings 98-10, pp. 298-300.

[7] H. Henke, "Design, measurement and manufacturing of mm-wave accelerating structures", 1999 Linear Collider Workshop, Frascati, 21-26 Oct. 1999.

[8] J. Cheng, Synchroton Radiation Research Center, Hsinchu, Taiwan.

[9] H. Henke, "Planar millimeter-wave RF structures", AIP Conf. Proc. 398 of the 7th Workshop Advanced Accelerator Concepts, Lake Tahoe, 1996.

[10] R. Apel and H. Henke, "Design of an on-axis coupled planar mm-wave structure", PAC 1999, Vol. 2, pp. 812-814.

[11] N.M. Kroll et al., "Planar accelerator structures for millimeter wavelengths", PAC 1999, Vol. 5, pp. 3612-14.

[12] M. Seidel, M. Hill and D.H. Whittum, "Subharmonic drive experiment at w-band in the NLCTA", SLAC, ARDB 125, 1997.

[13] P.B. Wilson, "Scaling linear colliders to 5TeV and above", SLAC-PUB-7449, April 1997.

[14] G. Caryotakis et al., "W-band micro-fabricated modular klystrons", SLAC-PUB-7624, Aug. 1997.

[15] G. Caryotakis et al., "High power w-band klystrons", Proceedings of the RF Workshop, Pajero Dunes, 5 - 9 Oct., 1998

[16] S. Solyga and H. Henke, "Two-dimensional design of a low-voltage mm-wave sheet beam klystrn", ITG Conference: Displays and Vacuum Electronics, Garmisch-Partenkirchen, Germany, April 29-30, 1998.

[17] E.R. Colby et al., "W-band sheet beam klystron simulation", SLAC, ARDB note 195.

[18] M. Blank et al., "Experimental investigation of w-band (93 GHz) gyroklystron amplifiers", IEEE Trans. on Plasma Science, Vol. 26, No. 3, June 1998, pp. 409-415.

[19] W. Lawson et al., "Design of a 10 MW, 91.392 GHz gyroklystron for advanced accelerators," this conference